Vibrational and low-energy optical spectra of the square-planar $Pd_3(PS_4)_2$ thiophosphate

C. Calareso, V. Grasso, and L. Silipigni
Dipartimento di Fisica della Materia e Tecnologie Fisiche Avanzate, Universitá di Messina, Salita Sperone 31, I-98166 Messina, Italy and Instituto Nazionale per la Fisica della Materia-Unitá di Messina, Messina, Italy
(Received 3 March 1998)

Room-temperature absorption and reflectance measurements have been carried out on single crystals of $Pd_3(PS_4)_2$ in the region from 1 to 5.5 eV. The resulting spectra have been interpreted on the basis of the analogies with those of other palladium compounds and within the framework of a simple molecular-orbital scheme. From the absorption spectrum analysis an optical gap of 2.12 eV has been deduced in good agreement with the literature. Below the fundamental absorption edge three weak structures have been observed and have been assigned as *d-d* spin-forbidden transitions. These features are also weakly visible in the reflectance spectrum. At photon energies greater than the absorption threshold the reflectance spectrum also presents three structures, the first more intense than the others. These bands have been identified as ligand-to-metal charge transfer transitions. Infrared and Raman spectra have also been measured in the regions $(550 \div 200)\ cm^{-1}$ and $(550 \div 100)\ cm^{-1}$, respectively. The observed vibrational spectra, interpreted on the basis of both the symmetry properties and the comparison with those of other palladium and $(PS_4)^{3-}$ containing compounds, well agree with the x-ray crystal structure data. Evidence of the slightly distorted tetrahedral $(PS_4)^{3-}$ unit presence and of a covalent character for the Pd-S bond has been obtained. [S0163-1829(99)04228-9]

INTRODUCTION

The palladium thiophosphate, represented by the chemical formula $Pd_3(PS_4)_2$, is a member of the M_xPCh_4 compound family, where M is a metal, P is phosphorous, Ch is a chalcogen, in particular S or Se, and the subscript x is equal to 3 with $M=$Cu, 1.5 with $M=$Pd, Co, Hg, Sr, W and 1 with $M=$B, Al, Ga, In, Bi, Cr. In all these compounds the phosphorus atom is exclusively in tetrahedral S coordination constituting thus the PS_4 group. The presence of strong P-S bonding within the PS_4 cluster, indicated by an average bond length of 2.03 Å, classifies these compounds as thiophosphates.[1]

Within such a large family, $Pd_3(PS_4)_2$ containing the palladium, a well-known catalyst, may provide surfaces on which photocatalytic reactions can take place.[2] This possibility has supposed the utility of this compound as a catalytic photoelectrode in photoelectrochemical, photovoltaic and electrophotosynthetic cells. Moreover, $Pd_3(PS_4)_2$ has been described as a diamagnetic semiconductor with a resistivity of about $4\times10^6\ \Omega$ cm at room temperature and an optical band gap ΔE of about 2.2 eV.[3] Therefore, in $Pd_3(PS_4)_2$ the semiconductivity and catalytic properties combine. This intrinsic capacity, which is one of the basic properties that makes a given single crystal a suitable electrode material for regenerative photovoltaic and photoelectrolysis devices, has led to an investigation of its photoelectronic properties.

In particular, the photoelectrochemical characterization[4] of $Pd_3(PS_4)_2$ has shown that this compound exhibits appreciable photoeffects in a number of solutions, showing the best results in I^- and Br^- electrolytes. From the analysis of the band edge a value of 2.54 eV results for the band gap (indirect) and there is also an indication of a direct gap at 2.89 eV. Therefore, a large difference between the value of 2.15 eV, deduced for the optical gap from absorption measurements,[4] and the photoelectrochemically measured indirect transition has been observed. This discrepancy has been ascribed to the low mobility of carriers in this material that seems to be related to the $Pd_3(PS_4)_2$ physical and electronic structure.

Crystallographic data[3,5] show the structure of $Pd_3(PS_4)_2$ to be trigonal with space group $P\bar{3}m1$ (D_{3d}^3): Pd^{2+} cations and $(PS_4)^{-3}$ anions form a network with an anti-Claudetite (As_2O_3)-type structure. Only by considering the main bonds, this material can be described as $Pd_3^{II}(P^+S_3S^-)_2$. The coordination polyhedron around the P atom is a trigonal pyramid rather than a tetrahedron with three distances P-S$=2.10$ Å and the fourth P-S$^-=2.0$ Å. The covalently bound S atoms have 1P+2Pd neighbors, which together with the lone electron pair form a distorted tethraedron. Each Pd atom is surrounded by four S atoms of two PS_4 tetrahedra in an essentially square-planar configuration. This is the favorite arrangement of ligands for the Pd^{2+} ion. The $[PdS_4]$ square appears to be fairly regular with Pd-S$=2.32$ Å. Other two sulfur atoms of two PS_4 units complete the coordination picture around each Pd atom in a very distorted elongated octahedron. The layers are weakly held together electrostatically by the singular S^- ions: the S^--Pd and S^--S distances to the next layer are 3.59 and 3.85 Å, respectively.

Even if $Pd_3(PS_4)_2$ shows itself as a candidate electrode material in photoelectrochemical cells, as far as we are aware, the experimental information concerning its physical properties is rather scarce: no detailed study of its vibrational, optical, and electronic properties has been reported. Such an investigation is essential for understanding the electronic structure of this compound, which is not yet known, and for supposing other possible technological applications.

The aim of this paper is twofold: to deduce more detailed information about both the electronic structure and the bond nature of $Pd_3(PS_4)_2$. Therefore, we present the room temperature absorption and reflectance spectra obtained in the region from 1 to 5.5 eV. These spectral data have been compared with those of other palladium compounds and inter-

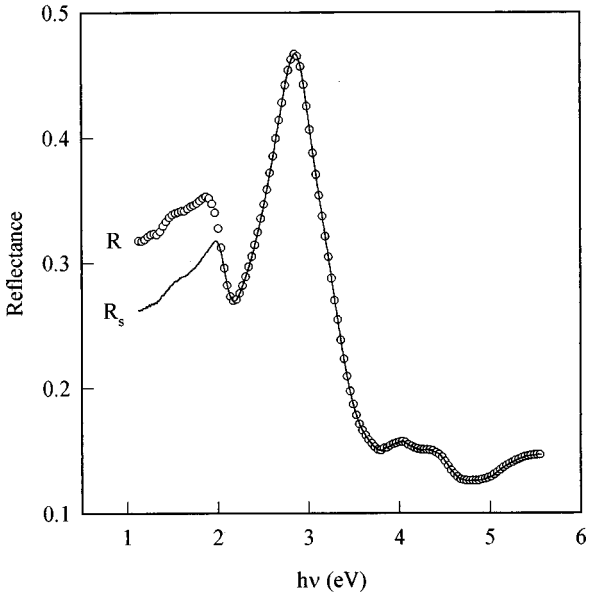

FIG. 1. Room temperature reflectance spectrum of a $Pd_3(PS_4)_2$ single crystal. The open circles represent the experimental R data; the solid line is the calculated one-surface reflectance R_s.

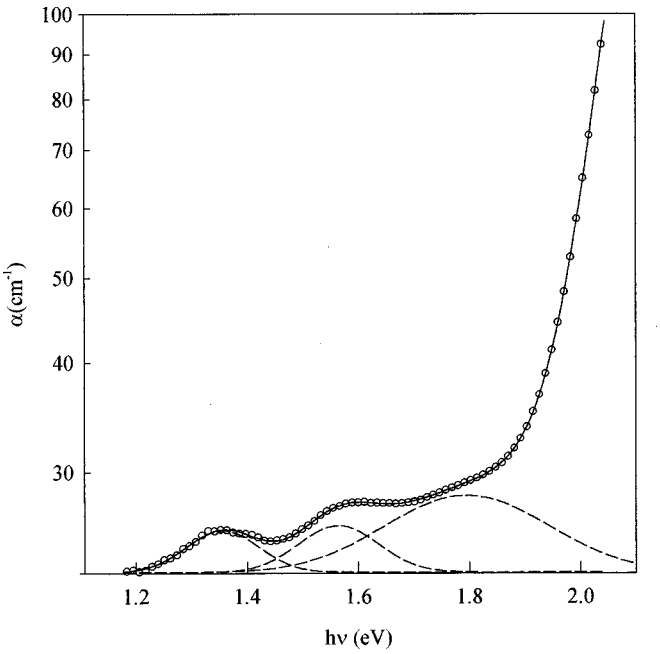

FIG. 2. Room-temperature optical absorption spectrum of a 200 μm $Pd_3(PS_4)_2$ single crystal in the region of the Pd $4d$-$4d$ transitions. The open circles represent the absorption coefficient α calculated from the absorbance and true reflectance data according to Eq. (3) in Ref. 7, the solid line is the best fit calculated absorption spectrum, while the dashed lines are the Gaussian curves.

preted within a simple molecular orbital scheme. We also show the $Pd_3(PS_4)_2$ infrared and Raman spectra recorded in the $(550 \div 200)$ cm^{-1} and $(550 \div 100)$ cm^{-1} regions, respectively. The assignment of the observed vibrational frequencies is based on both the symmetry properties and the comparison with the vibrational spectra of other palladium and $(PS_4)^{3-}$ compounds.

EXPERIMENTS

Room-temperature absorption and reflectance measurements were performed on single crystals of $Pd_3(PS_4)_2$ using a Perkin-Elmer double-beam UV-VIS spectrophotometer, model Lambda 2. In both cases unpolarized light struck the crystal surface at normal incidence. For the reflectance measurements a specular accessory was mounted. The investigated spectral region was between 1 and 5.5 eV.

Room-temperature infrared transmission spectra of $Pd_3(PS_4)_2$ single crystals were recorded on a Perkin-Elmer spectrophotometer, model 983, in the $(550 \div 200)$-cm^{-1} spectral range. A Dilor LabRam fast analytical micro-Raman spectroscopy system, equipped with a 15-mW He-Ne laser ($\lambda = 633$ nm), a notch filter and a two-dimensional charge coupled device detector, was used to measure the room-temperature Raman spectra between 550 and 100 cm^{-1}.

The samples used in the experiments appeared as purplish red plates with thickness in the range $d = (40 \div 200)$ μm. They were grown and supplied by Laboratoire de Physique des Matériaux Electroniques of the Institut de Physique Appliquée of the Ecole Polytechnique Fédérale de Lausanne. All of the measurements were repeated several times to check for their reproducibility.

RESULTS

In Fig. 1, the open circles represent the reflectance R of the $Pd_3(PS_4)_2$ single crystal, measured at room temperature and at normal incidence. Near the fundamental absorption edge, a pronounced rise in the reflectance spectral response R is observed. A similar reflectance increase is common to most layertype materials: it is a consequence of multiple reflections between the front and rear plane boundaries of sample.[6] In the absence of interference fringes, we have calculated the $Pd_3(PS_4)_2$ true reflectance R_s (the fraction of incident radiation that is reflected from the first surface) from the measured reflectance R and transmittance T data with the method reported in the literature.[7,8] The one-surface reflectance R_s of $Pd_3(PS_4)_2$, obtained in this way and represented in Fig. 1 with solid line, exhibits a residual increase around 1.98 eV followed by a very strong peak at about 2.86 eV and two weak structures at about 4.02 and 4.38 eV. For photon energies smaller than 1.90 eV some weak shoulders are visible. Since they are located in the spectral region where the correction for back reflection works well and because of their low intensity an accurate placement of these structures cannot be realized. However, a comparison with the absorption data reported in Fig. 2, allows us to identify only their nature as will be discussed later on. In Table I, the above-mentioned reflectance structures of $Pd_3(PS_4)_2$ are listed and identified.

As in the case of the $Cd_2P_2X_6$ and $Hg_2P_2X_6$ compounds,[7,8] we have calculated the absorption coefficient α of a 200-nm thick $Pd_3(PS_4)_2$ sample directly from the measured values of absorbance and true reflectance. The α room-temperature spectral variation is shown, below the fundamental absorption edge, in Fig. 2: three broad shoulders centered at about 1.36, 1.56, and 1.80 eV respectively, followed by a rising strong absorption beginning at energies higher than 1.90 eV can be distinguished. The three bands show an increasing intensity in the direction of higher energy of absorption. The steep absorption may mask further struc-

TABLE I. Assignments of the observed $Pd_3(PS_4)_2$ reflectance structures.

Transition energy (eV)	Assignment
<1.90	singlet-triplet d-d transitions
1.98	$^1A_{1g}\rightarrow{}^1A_{2g}$ and scattering by cleavage planes within the sample
2.86	$L\pi\rightarrow d$ charge-transfer and d-d spin-allowed transitions
4.02	$L\pi$-d charge-transfer transitions
4.38	$L\pi$-d charge-transfer transitions

tures, the presence of which may be emphasized by means of low-temperature absorption measurements. Since no vibronic structure is evident, we have analyzed the above-mentioned spectrum assuming that it can be represented as the sum of three overlapping Gaussian curves in the low-energy region and with an exponential function at higher energies. This decomposition is based, as will be discussed later on, on the analogy with the absorption spectra of other diamagnetic palladium complexes where, because of the palladium appreciable spin-orbit coupling, it is possible to observe weak d-d transitions below the fundamental absorption edge. The results of this analysis are given in Table II. In Fig. 2 the open circles represent the calculated α data, the dashed lines the obtained Gaussian curves, and the solid line the best fit calculated by means of a least-square fitting procedure. In Table III the assignments of the observed absorption structures and the fundamental absorption edge are tabulated.

Figure 3 shows the room-temperature $Pd_3(PS_4)_2$ infrared (curve a) and Raman (curve b) spectra in the $(550 \div 100)$-cm^{-1} spectral range. The observed vibrational frequencies, their relative intensities and the proposed assignments are summarized in Table IV, where the fundamental frequencies of the tetrahedral free $(PS_4)^{3-}$ ion are also listed for comparison. Between 550 and 400 cm^{-1} the infrared spectrum (curve a) exhibits a very strong feature positioned at about 492 cm^{-1}, a shoulder at about 512 cm^{-1}, and a weak band located around 413 cm^{-1}. At lower frequencies three rather intense bands occur: the first structure consists of two overlapping bands positioned at about 317 and 296 cm^{-1}; the second one, characterized by a medium intensity, appears at about 263 cm^{-1} and the third one is located at about 234 cm^{-1}. As one can see in Fig. 3 and in Table IV, the comparison of Raman and infrared spectra shows that some Raman bands present an infrared counterpart. Below 400 cm^{-1}

TABLE II. Energies of the absorption maxima E_0, heights of the maxima (in cm^{-1}) A and half widths σ of the Gaussian curves $A\times\exp\{-\ln(2)[(\hbar\omega-E_0)/\sigma]^2\}$ used to fit the absorption peaks of the palladium $4d$-$4d$ spin-forbidden transitions in $Pd_3(PS_4)_2$. E_g is the fundamental absorption edge.

E_0 (eV)	A (cm^{-1})	σ (eV)	E_g (eV)
1.36	25.72	0.07	2.12
1.56	26.06	0.08	
1.80	28.22	0.17	

TABLE III. Assignments of the observed absorption structures and fundamental absorption edge, whose energy positions are denoted with E_i ($i=1$, 2, 3, and g in order of increasing energy).

E_i (eV)	Assignment
1.36	singlet-triplet d-d transition
1.56	singlet-triplet d-d transition
1.80	singlet-triplet d-d transition
2.12	$L\pi\rightarrow d$ charge-transfer transition

the strongest Raman features occur: a sharp line at about 311 cm^{-1} and a very strong doublet consisting of two narrow lines positioned at about 191 and 186 cm^{-1}. A weak and rather broad structure, due to an overlap of two bands at about 249 and 237 cm^{-1} is also present, as better shown in the enlargement of the Raman $(260 \div 230)$-cm^{-1} spectral range (see curve b').

DISCUSSION

As already said in the introduction, the crystallographic data indicate that in $Pd_3(PS_4)_2$ palladium is present as a bivalent cation. Consequently the Pd^{+2} ion has a $4d^8$ electronic configuration. Moreover $Pd_3(PS_4)_2$ is a square-planar d^8 palladium complex: even if there are six sulfur atoms around each palladium cation, the local symmetry about Pd^{2+} is not octahedral (O_h) but tetragonal (D_{4h}), i.e., four sulfur atoms are arranged in a square at whose center the palladium cation is located while two other sulfur atoms are placed above and below this plane. This arrangement is characteristic of bivalent palladium and makes diamagnetic the $Pd_3(PS_4)_2$ compound, as shown from a magnetic study.[3] The octahedral field, imposed by the six sulfur atoms, splits the five d orbitals, degenerate in the free ion, into a triply degenerate t_{2g}

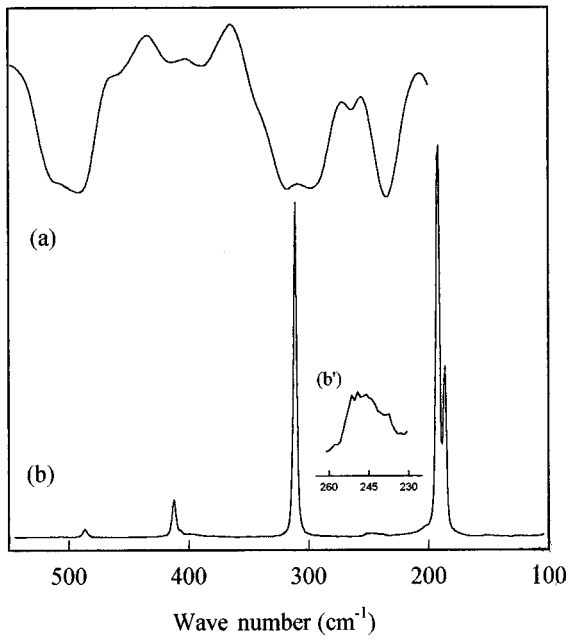

FIG. 3. The $Pd_3(PS_4)_2$ infrared (a) and Raman (b) spectra obtained at room temperature in the spectral range $(550 \div 100)$ cm^{-1}. The curve (b') is an enlargement of the Raman spectrum between 260 and 230 cm^{-1}.

TABLE IV. The $Pd_3(PS_4)_2$ infrared and Raman frequencies (cm^{-1}), their relative intensities and proposed assignments in comparison with the ''free'' $(PS_4)^{3-}$ ion vibration modes (Ref. 23). s=strong, m=medium, w=weak, sh=shoulder, br=broad, v=very.

$Pd_3(PS_4)_2$ IR	$Pd_3(PS_4)_2$ Raman		$(PS_4)^{3-}$ (Ref. 23) (T_d)	Assignments
	186s-m			δ(S-Pd-S)
	191vs		215 $\nu_2[E(R)]$	δ_d(S-P-S)
234s	237w			
263m		>	270 $\nu_4[F_2(R,\mathrm{IR}]$	δ_d(S-P-S)
	249w			ν_{as}(Pd-S)
	311s			ν_s(Pd-S)
296vs		>		ν_d(Pd-S)
317vs				
413w	412m		416 $\nu_1[A_1(R)]$	ν_s(P-S)
492vs	487m-w	>	548 $\nu_3[F_2(R,\mathrm{IR})]$	ν_d(P-S)
512sh				

orbital set and into a doubly degenerate e_g orbital set. The lowering of symmetry from O_h to D_{4h} causes a further splitting of the d orbitals into four different levels, the ordering of which may depend on the metal ion and the type of ligand under consideration.

Figure 4 shows the possible orderings of the $4d$ orbital energies as a tetragonal distortion is applied to an octahedral coordination: the triply degenerate t_{2g} orbital set are given by the functions d_{xy}, d_{xz}, and d_{yz}, while the doubly degenerate e_g orbitals set by $d_{x^2-y^2}$ and d_{z^2}.[9] As an increasing tetragonal distortion is impressed upon the system the possible arrangements A, B, and C arise: a_{1g}, b_{1g}, b_{2g}, and e_g are the symmetry types in which the central metal ion d_{z^2}, $d_{x^2-y^2}$, d_{xy}, and d_{xz},d_{yz} orbitals transform, respectively, in the point group D_{4h}. As regards the s, p_x, p_y, and p_z orbitals of the central metal ion the a_{1g}, e_u, and a_{2u} symmetry types are expected.[10]

Since to our knowledge no theoretical or experimental information about the $Pd_3(PS_4)_2$ electronic band structure exists, we may interpret the reflectance and absorption spectra reported in Figs. 1 and 2, respectively only by comparison with those of other palladium compounds.

It is known that the optical spectra of most transition metal compounds are characterized by two groups of possible transitions: (i) excitations between the incomplete outer d orbitals of the transition-metal ion and (ii) others, comprising ligand-to-metal, metal-to-ligand, intrametal, or intraligand transitions. The former are all parity forbidden and therefore weak; the latter can be both weak and strong. For most octahedral complexes of the transition metals the nature of the weak, long-wavelength absorption bands is well understood and detailed assignments to transitions within the d^n configuration of the metal ion have been made. The corresponding problem for planar complexes is more difficult since the effect of the ligands on the energies of the different d orbitals is much more complicated. Various molecular-orbital approaches have been used for the interpretation of the electronic spectra of some square planar palladium complexes.[10–15] However, as far as the low-intensity d-d

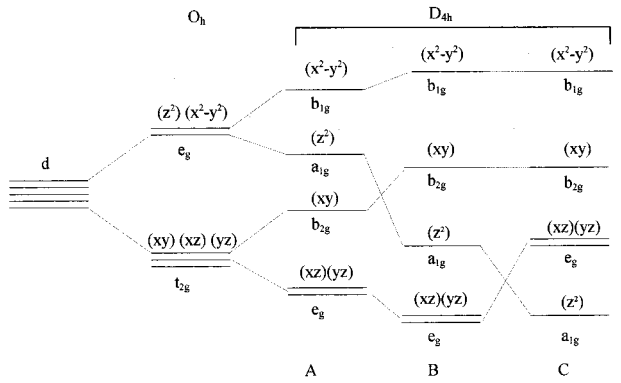

FIG. 4. Possible arrangement of the d orbitals in a complex with D_{4h} symmetry. Degeneracies under the octahedral splitting are further broken as a tetragonal distortion, increasing toward the right, is applied.

transitions are concerned, there seems to be the general agreement that the ''d-like'' molecular orbital ordering is

$$b_{1g}(d_{x^2-y^2}) > b_{2g}(d_{xy}) > e_g(d_{xz,yz}) > a_{1g}(d_{z^2}),$$

in agreement with the C arrangement of Fig. 4. If we adopt the same d molecular-orbital's level ordering for $Pd_3(PS_4)_2$ and since the Pd^{+2} ion is diamagnetic, its ground state is $^1A_{1g}$ with the $d_{x^2-y^2}$ orbital utilized for bonding and the eight electrons, which occupy the four other d orbitals.[16] If we also assume that in $Pd_3(PS_4)_2$, as happens in other square planar palladium complexes,[12] the highest occupied levels and the lowest unoccupied level are mainly metal d orbitals, the lowest unfilled molecular orbital is then the antibonding orbital involving $d_{x^2-y^2}$ with b_{1g} symmetry. In this way the optical spectra of $Pd_3(PS_4)_2$, in analogy with those of other diamagnetic palladium complexes,[12,14–19] should show at low energies d-d transitions, that is transitions in which electrons from the d filled orbitals are excited to the b_{1g}^* orbital. These transitions, which are based mainly on the metal, are designated as follows:

$$d_{z^2} \rightarrow d_{x^2-y^2}, \quad {}^{1,3}B_{1g}; \quad d_{xy} \rightarrow d_{x^2-y^2}, \quad {}^{1,3}A_{2g};$$
$$d_{xz,yz} \rightarrow d_{x^2-y^2}, \quad {}^{1,3}E_g,$$

where, for example, by $d_{xy} \rightarrow d_{x^2-y^2}$ we denote the subconfiguration arising from the ground-state configuration by the promotion of an electron from the d_{xy} to the $d_{x^2-y^2}$ orbital. Near each transition the symmetry of the excited state is also indicated. Since palladium, like platinum, shows an appreciable, even if lower, spin-orbit coupling,[17] it is possible to observe not only the singlet-singlet d-d transitions but also the singlet-triplet d-d ones. Even if all these transitions are less intense than the charge-transfer ones, the singlet-triplet d-d excitations show a lower intensity: they are at least an order of magnitude weaker.[9] Moreover, the singlet-singlet d-d transitions are spin allowed but parity forbidden as electrical dipole transitions. Therefore, even if characterized by low intensity, they are visible because they borrow intensity from higher allowed transitions by vibronic perturbations.[16] The singlet-triplet d-d transitions are spinforbidden and located at lower energies than the corresponding singlet-singlet d-d transitions.[10]

In the light of these observations, we assign the weak bands positioned at 1.36, 1.56, and 1.80 eV in the $Pd_3(PS_4)_2$ absorption spectrum (see Fig. 2) to the singlet-triplet d-d spin-forbidden transitions. Only on the basis of a comparison with the optical spectra of other palladium compounds an identification of the individual states in the triplets is not feasible since, because of the palladium smaller spin-orbit coupling, the singlet-triplet d-d spin-forbidden transitions are not always visible in the spectra. As already said, each singlet-triplet excitation has a corresponding singlet-singlet one at higher energy. If in $Pd_3(PS_4)_2$, as happens in some palladium and platinum compounds,[10–12] the singlet-singlet d-d transition appears at about 1 eV or less from the corresponding singlet-triplet band, the singlet-singlet d-d bands will be not visible in Fig. 2 as they are obscured by the rising strong absorption beginning at energies higher than 1.90 eV. The position of 2.12 eV for the $Pd_3(PS_4)_2$ band edge, deduced by the best fit, well agrees to that reported in the literature.[4] On the basis of the absorption edge definition in semiconductor or insulator transition-metal compounds, the obtained $Pd_3(PS_4)_2$ band edge may be associated with a ligand-to-metal or metal-to-ligand charge-transfer transition.[36]

As regards the $Pd_3(PS_4)_2$ reflectance measurements, the pronounced rise observed near the absorption edge in Fig. 1 is common to most layertype materials and can be explained as being partially due to the back surface reflection resulting in multiple reflection within the sample.[6,20] However, as shown in Fig. 1, the correction for the back reflection reduces the rise in reflectance but does not remove it completely. This residual increase can be the result of either or both of two concomitant causes. The first one is, in agreement with the literature, the scattering caused by the cleavage planes within the sample which are parallel to its surfaces.[20] The second possible cause is the presence of a structure associated with the d-d transitions. In fact, the optical spectra of some palladium compounds, such as K_2PdCl_4 and K_2PdBr_4,[21] show a peak at about 1.98 eV due to the first d-d spin-allowed transition, that is the $^1A_{1g} \rightarrow {}^1A_{2g}$ or $b_{2g}(xy) \rightarrow b_{1g}^*(x^2-y^2)$ transition.

In the above-mentioned hypothesis that in $Pd_3(PS_4)_2$ the highest occupied levels and the lowest unoccupied level are mainly metal d orbitals, the high-intensity band located at about 2.86 eV may be assigned to ligand-to-metal charge-transfer transitions ($L\pi \rightarrow d$). The same nature may be associated to the optical band gap of 2.12 eV, which does not show any structure in R_s if we suppose, as reported in the literature, an indirect nature for it. Moreover, the feature at 2.86 eV well agrees with the value of 2.89 eV reported in the literature for a direct gap in $Pd_3(PS_4)_2$.[4] In the spectral region below 1.90 eV some weak shoulders appear in the reflectance of Fig. 1. Because of their low intensity, they are not well defined but a comparison with the absorption spectrum reported in Fig. 2 identifies them as the singlet-triplet d-d spin-forbidden transitions. Since a d-d spin-allowed transition is associated to each a d-d spin-forbidden one with the first transition positioned at higher energies, the charge-transfer band at about 2.86 eV could mask those spin-allowed d-d bands which should be located between 2.00 and 3.75 eV.[13,14,21]

As regards the weak structures around 4.02 and 4.38 eV, the first is separated from the high-intensity band around 2.86 eV by about 1.34 eV. This energy separation well agrees with that observed in some square-planar halide complexes, where two charge transfer bands, separated by 1.24 to 1.61 eV with the second more intense than the first, are observed.[21] The different intensity ratio may be due to the fact that the other two d-d spin-allowed transitions can contribute to the peak around 2.86 eV. The comparison with the K_2PdBr_4 optical spectra, in which a minor peak is observed at 4.60 eV,[15] suggests that the weak shoulder around 4.38 eV might also be due to ligand-to-metal charge-transfer transitions. At present no conclusions are possible regarding the nature of the ligand states involved in these transitions. This needs an accurate band-structure calculation or at least a semiempirical energy level scheme, which may be used as a basis for the interpretation of the experimental results.

With respect to the $Pd_3(PS_4)_2$ infrared and Raman spectra, according to the reported structural determination,[3,5] the building elements are discrete $[PS_4]^{3-}$ anions, which are linked by the Pd^{2+} cations. Since the Pd-S and P-S bonding distances are closely covered by the sum of the corresponding covalent radii (Pd 1.28 Å, P 1.10 Å, S 1.04 Å), the existence of the Pd-S and P-S covalent bonds can be supposed. Therefore, in $Pd_3(PS_4)_2$ two units can be recognized: PS_4 and PdS_4. On the basis of the ''site symmetry'' group analysis for the tetrahedral PS_4^{3-} unit (T_d symmetry) and the planar PdS_4 one (D_{4h} symmetry) (Refs. 22–27) and by comparison with the vibrational spectra of both other $[PS_4]^{3-}$ containing compounds and some palladium square-planar complexes,[22–32] we have interpreted the Raman and infrared spectra of Fig. 3 as follows. The bands located between 550 and 400 cm^{-1} can be described in terms of the P-S vibrational stretching modes by analogy with the vibrational spectra of the MPS_4 (M = In, Ga, Bi) (Ref. 28) and Na_3PS_4 (Ref. 22) compounds. In particular, the strong infrared band at about 492 cm^{-1} as well as the shoulder at about 512 cm^{-1} has been assigned to the $\nu_3(F_2)$ mode resulting from a degenerate P-S stretching vibration, ν_d(P-S). This mode of vibration is reported for the free $[PS_4]^{3-}$ ion at 548 cm^{-1},[23] as shown in Table IV. The observation of two infrared components suggests degeneracy removing probably due to a lowering of symmetry. As a matter of fact the $Pd_3(PS_4)_2$ structural data analysis reports the presence of slightly distorted tetrahedral $[PS_4]^{3-}$ groups and a ''2d'' position, in the Wyckoff notation, for the P atoms.[3,5] In the D_{3d}^3 space group the d position corresponds to a C_{3v}-point symmetry.[34] Therefore, in the authors' opinion the split of the $\nu_3(F_2)$ degenerate mode can be attributed to a lowering of symmetry from T_d to C_{3v} for the $[PS_4]^{3-}$ group. The Table V, which is the $T_d \rightarrow C_{3v}$ correlation one, supports this assignment. As shown in Fig. 3, curve b, the $\nu_3(F_2)$ degenerate mode presents a weak Raman counterpart at about 487 cm^{-1} as expected. The observed weak intensity also seems to indicate a small coupling between two $[PS_4]^{3-}$ units by correlation effects. Such an hypothesis agrees well with the $Pd_3(PS_4)_2$ structural data according to which the $[PS_4]^{3-}$ anions are linked by the Pd^{2+} ions.[3,5] The lowering of symmetry from $T_d \rightarrow C_{3v}$ is also confirmed by the presence of the weak infrared band at about 413 cm^{-1}. In fact, this feature, which

TABLE V. The $T_d \rightarrow C_{3v}$ correlation table.

Point group	ν_1	ν_2	ν_3	ν_4
T_d	$A_1(R)$	$E(R)$	$F_2(I,R)$	$F_2(I,R)$
C_{3v}	$A_1(I,R)$	$E(I,R)$	$A_1(I,R)+E(I,R)$	$A_1(I,R)+E(I,R)$

presents a strong Raman counterpart at the same frequency, can be ascribed to the $\nu_1(A_1)$ mode deriving from a symmetric stretching vibration of the P-S bond, ν_s(P-S), in the $[PS_4]^{3-}$ ion. The ν_1 mode is only Raman active in the T_d symmetry, but it becomes infrared active if the symmetry is lowered to C_{3v} as happens in $Pd_3(PS_4)_2$. Moreover, as one can see in Table IV, this mode is not very sensitive to the cation in good agreement with the literature.[33] The other infrared and Raman structures observed at lower frequencies can be attributed to either the S-P-S bending vibrations in the (PS_4) units or the Pd-S vibrations in the (PdS_4) group.

With respect to the S-P-S bending vibrations in the (PS_4) group, the infrared structures at about 263 and 237 cm^{-1}, of medium and strong intensity, respectively, show the same behavior as the strong band and shoulder observed at about 492 and 512 cm^{-1} in the stretching region. In fact, they have a weak Raman counterpart at about 237 cm^{-1}, whose presence has been emphasized in the curve b'. Therefore, on the basis of this analogy and by comparison with other $[PS_4]^{3-}$ containing compounds, these infrared and Raman structures can be attributed to the $\nu_4(F_2)$ mode resulting from a degenerate S-P-S bending vibration, δ_d (S-P-S). The presence of two infrared components confirms degeneracy removing due to the above-supposed lowering of symmetry. The very strong Raman feature at about 191 cm^{-1}, whose possible infrared counterpart has not been detected since it probably lies below 200 cm^{-1}, can be identified with the $\nu_2(E)$ mode derived from a degenerate S-P-S bending. This attribution is in good agreement with the literature according to which the $\nu_2(E)$ mode is stronger and at lower frequencies than $\nu_4(F_2)$.[24,25]

As regards the Pd-S vibrations in PdS_4 groups, some of them, in particular the Pd-S stretching modes, have been observed in some palladium and sulfur compounds at $(350 \div 300)\ cm^{-1}$.[35] Therefore, the strong infrared bands observed at about 317 and 296 cm^{-1} can be attributed to the $\nu_6(E_u)$ degenerate Pd-S stretching mode, ν_d(Pd-S), which has no Raman counterpart. The presence of two components seems to indicate degeneracy removing due to a site effect. This is possible since, according to the structural data the Pd atoms occupy a ''3*e*'' positions in $Pd_3(PS_4)_2$.[3,5] In the D^3_{3d} space group, a C_{2h}-point symmetry corresponds to these positions,[34] therefore a lowering of symmetry from D_{4h} to C_{2h} is possible for the PdS_4 groups. The other infrared active modes, $\nu_7(E_u)$ and $\nu_3(A_{2u})$, cannot give rise to any structure in our infrared spectrum having been observed in other palladium complexes below 200 cm^{-1}.[26] On the contrary, all the expected Raman modes, related to the Pd-S vibrations, appear. In fact, the $\nu_1(A_{1g})$ symmetric Pd-S stretching mode, ν_s(Pd-S), which is only Raman active, is identified with the Raman sharp line positioned at about 311 cm^{-1}. This assignment is supported by the analogy with the vibrational spectra of other palladium compounds.[29] Similarly the weak Raman band located at about 249 cm^{-1}, which has not an infrared counterpart, can be attributed to the $\nu_4(B_{2g})$ asymmetric Pd-S stretching mode, ν_{as}(Pd-S). Finally the strong Raman line located at about 186 cm^{-1} is due to the $\nu_2(B_{1g})$ in-plane S-Pd-S deformation mode. On the basis of these attributions, we observe the following Raman frequency sequence:

$$\nu_1(A_{1g}) > \nu_4(B_{2g}) > \nu_2(B_{1g}),$$

which is in agreement with that reported in other square-planar palladium compounds, such as K_2PdCl_4 and K_2PdBr_4.[26] Moreover, as expected the ν_6 mode lies at higher frequencies than the ν_1 one.[24,26]

CONCLUSIONS

In this paper we have analyzed the optical and vibrational properties of the $Pd_3(PS_4)_2$ thiophosphate. The deduced information can be summarized as follows.

From the analysis of the room-temperature reflectance spectrum of $Pd_3(PS_4)_2$ it results that two different band systems can be identified, namely the weak *d*-*d* bands below the fundamental absorption threshold and the high-intensity ligand-to-metal charge transfer bands at higher photon energies. The highest ligand-to-metal band seems to derive also from some *d*-*d* spin allowed transitions.

The study of the room-temperature absorption spectrum below the fundamental threshold confirms the presence of the *d*-*d* spin-forbidden transitions and classifies this compound as a broad band semiconductor with an optical gap of 2.12 eV. This band gap, whose value and nature are in good agreement with the literature, is associated to a ligand-to-metal charge-transfer transition.

As regards the $Pd_3(PS_4)_2$ Raman and infrared spectra, two covalent units, PS_4 and PdS_4, can be recognized in good agreement with the existing crystallographic data. Site effects seem to be operative on both groups, which show some deviations from their ideal symmetry. The P-S vibrational stretching modes are observed in the $(520 \div 400)\ cm^{-1}$ spectral range, while below 400 cm^{-1} the observed features are assigned to the S-P-S bending modes and the Pd-S stretching and S-Pd-S bending modes.

ACKNOWLEDGMENTS

We wish to thank H. Berger and Professor G. Margaritondo of the Institut de Physique Appliquée of the École Polytechnique Fédérale de Lausanne for supplying the investigated $Pd_3(PS_4)_2$ crystals. We also thank Dr. N. Oddo and Dr. R. Valisa of the Instruments S.A. Italia for allowing the use of their micro-Raman spectroscopy system.

[1] R. Difhl and C. D. Carpentier, Acta Crystallogr., Sect. B: Struct. Crystallogr. Cryst. Chem. **34**, 1097 (1978).
[2] J. V. Marzik, R. Kershaw, K. Dwight, and A. Wold, Solid State Chem. **44**, 382 (1982).
[3] T. A. Bither, P. C. Donohue, and H. S. Young, J. Solid State Chem. **3**, 300 (1971).
[4] J. C. W. Folmer, J. A. Turner, and B. A. Parkinson, J. Solid State Chem. **68**, 28 (1987).
[5] A. Simon, K. Peters, E. M. Peters, and H. Hahn, Z. Naturforsch. B **38**, 426 (1983).
[6] A. M. Elkorashy, Phys. Status Solidi B **135**, 707 (1986).
[7] C. Calareso, V. Grasso, F. Neri, and L. Silipigni, J. Phys.: Condens. Matter **9**, 4791 (1997).
[8] C. Calareso, V. Grasso, and L. Silipigni, J. Appl. Phys. **82**, 6228 (1997).
[9] Don S. Martin, Jr. and C. A. Lenhardt, Inorg. Chem. **3**, 1368 (1964).
[10] J. Chatt, G. A. Gamlen, and L. E. Orgel, J. Chem. Soc. **1958**, 486.
[11] H. Basch and B. Gray, Inorg. Chem. **6**, 365 (1967).
[12] L. I. Elding and L. F. Olsson, J. Phys. Chem. **82**, 69 (1978).
[13] R. P. Messmer, L. V. Interrante, and K. H. Johnson, J. Am. Chem. Soc. **96**, 3847 (1974).
[14] W. R. Mason III and H. B. Gray, J. Am. Chem. Soc. **90**, 5721 (1968).
[15] R. M. Rush, Don S. Martin, Jr., and R. G. LeGrand, Inorg. Chem. **14**, 2543 (1975).
[16] M. L. Rodgers and Don S. Martin, Polyhedron **6**, 225 (1987).
[17] Don S. Martin, Jr., M. A. Tucker, and A. J. Kassman, Inorg. Chem. **4**, 1682 (1965).
[18] P. Day, M. J. Smith, and R. J. P. Williams, J. Chem. Soc. A **1968**, 668.
[19] P. Day, A. F. Orchard, A. J. Thomson, and R. J. P. Williams, J. Chem. Phys. **42**, 1973 (1965).
[20] A. M. Elkorashy, J. Phys. C **21**, 2595 (1988).
[21] H. B. Gray and C. J. Ballahausen J. Am. Chem. Soc. **85**, 260 (1963).
[22] M. M. Maurice, J. F. Leroy, G. Kaufmann, A. Muller et Herbert, W. Roesky, C. R. Seances Acad. Sci., Ser. C **267**, 563 (1968).
[23] A. Müller, N. Mohan, P. Cristophliemk, I. Tossidis, and M. Drägen, Spectrochim. Acta A **29**, 1345 (1973).
[24] K. Nakamoto, *Infrared Spectra of Inorganic and Coordination Compounds*, 2nd ed. (Wiley, New York, 1970), Sec. II.
[25] K. Nakamoto, *Infrared and Raman Spectra of Inorganic and Coordination Compounds*, 4th ed. (Wiley, New York, 1986), Pt. II.
[26] P. J. Hendra, J. Chem. Soc. A **1967**, 1298.
[27] K. Nakamoto, *Infrared Spectra of Inorganic and Coordination Compounds* (Ref. 24), Sec. I.
[28] V. S. D'Ordyai, I. V. Galagovets, E. Yu. Peresh, Yu. V. Varoschilov, V. S. Gerasimenko, and V. Yu. Slivka, Russ. J. Inorg. Chem. **24**, 11 (1979).
[29] J. R. Allkins and P. J. Hendra, J. Chem. Soc. A **1967**, 1325.
[30] A. Sabatini, L. Sacconi, and V. Schettino, Inorg. Chem. **3**, 1775 (1964).
[31] K. Chondrouds and M. G. Kanatzidis, Inorg. Chem. **36**, 5859 (1997).
[32] W. Brockener and U. Pätzmann, Z. Naturforsch. A **42**, 513 (1987).
[33] P. R. Mercier, J. P. Mahugani, B. Fahys, and G. Robert, Acta Crystallogr., Sect. B: Struct. Crystallogr. Cryst. Chem. **38**, 1887 (1982).
[34] *International Tables for X-ray Crystallography* Vol. 1 (Kynoch Press, England, 1965).
[35] K. Nakamoto, *Infrared Spectra of Inorganic and Coordination Compounds* (Ref. 24), Sec. III.
[36] M. Piacentiní, F. S. Khumals, G. Leveque, C. G. Olson, and D. W. Lynch, Chem. Phys. **72**, 61 (1982).